Asymmetric source acoustic LWD for the improved formation shear velocity estimation

Tianrun Chen, Bing Wang, Zhenya Zhu and Dan Burns, ERL, Department of Earth, Atmospheric and Planetary Sciences, MIT

SUMMARY

Most acoustic logging while drilling (LWD) tools generate a single pure borehole mode (e.g., dipole or quadrupole) to estimate the formation shear velocity. We propose an approach where multipole modes are generated simultaneously and used to obtain a better shear estimation. This approach uses an asymmetric source with arrays of receivers distributed azimuthally around the tool to generate and identify signals from different modes. We investigate such an approach using both synthetic and laboratory data. The laboratory data are collected from a scale-model LWD tool with one active source transducer mounted on the side of the tool. Four sets of receiver arrays, each separated by 90 degrees azimuthally, are used to isolate monopole, dipole and quadrupole modes by coherently adding and subtracting received arrivals. A method is then apply to perform dispersion analysis on these arrivals. With least square fitting, formation shear velocities are estimated from both dipole and quadrupole modes' arrivals. We find that, by averaging the estimates obtained independently from dipole and quadrupole modes, we can reduce the uncertainty and improve the confidence of the estimation for the formation shear velocity.

INTRODUCTION

Acoustic LWD tools have been designed with specific applications. One of these applications is to estimat the formation shear velocity, which can be quite challenging because higher order borehole modes, such as dipole and quadrupole, are dispersive and the phase velocity equals to the formation shear velocity only at the cutoff frequency. In the case of dipole logging, it is difficult to effectively generate this mode at frequency ranges that are low enough to close the cut-off frequency. The presence of a tool flexural mode that interacts strongly with the formation flexural mode in these frequency ranges further complicates the analysis and makes the interpretation of formation properties more difficult (Rao et al., 1999). Quadrupole logging has the advantage of not having an interfering tool screw mode to deal with, however the dispersion problem remains an issue as does the lower excitation energy of this mode. An additional complication exists if the tool is not centered in the borehole or the source transducers are not matched. In these situations, pure dipole or quadrupole mode will not be excited as both higher and lower order modes are also generated. Byun et al. (2004) and Byun and Toksoz (2006) studied the effects of source mismatch and off-center tools on the modes generated in acoustic LWD. Although the dipole or quadrupole mode could still be isolated by appropriate summation of receivers located around the tool circumference, Stoneley and higher order modes are also present in the time series.

These issues and complications in acoustic LWD tool could lead to significant errors in the estimated formation shear velocities. An example of such errors is given in Briggs et al. (2004), where a comparison of shear wave velocity measured by wireline and dipole LWD showed differences averaging 5-7%, with some zones showing differences greater than 10%. In general, there was a consistent bias with the LWD values being faster than the wireline values (Briggs et al., 2004). Although these disagreements could, in part, be due to the fact that the wireline data was collected 10 days later than the LWD data allowing some time for alteration and invasion effects to take place, it is more likely that the bias is due to mode impurity in the LWD data and resulting uncertainty in dispersion corrections applied to the measurements.

These observations and previous studies suggest another approach to estimate shear velocity. Rather than focus on generating a single pure borehole mode (e.g., dipole, quadrupole, etc) and estimating the shear velocity from that mode, we generate several modes each with different sensitivity to the shear velocity over different frequency bands and average the estimated results from all the modes to reduce uncertainty and improve the confidence of the estimation. We propose using an asymmetric source, that is a single source on one side of the tool, together with arrays of receivers distributed azimuthally around the tool to allow different modes to be identified and analyzed. We investigate this approach using both synthetic and laboratory data. The laboratory data uses a scale-model LWD tool as described in Zhu et al. (2008) with one active sources transducer mounted on the side of the tool. This source geometry simultaneously generates all borehole modes with different amplitudes. We use four sets of receiver arrays each separated by 90 degrees azimuthally to isolate and analyze monopole, dipole and quadrupole modes by coherently adding and subtracting the signals received from different receiver arrays. We then apply a method of estimating the dispersion curves from time series data developed by Rao and Toksoz (2005). This method estimates the phase velocities of the monopole, dipole and quadrupole modes at different frequency ranges through the use of a series of narrow bandpass filters combined with a time semblance analysis by Kimball and Marzetta (1986). With this approach, a dispersion correction could be used to estimate the formation shear velocity when the frequency range of the measurements does not include the cut off frequency for each individual mode. We apply the least square fitting to estimate formation shear velocity from each individual mode's arrivals, and finally average the estimated results from all the modes to obtain the estimate for the formation shear velocity.

METHODOLOGY

In this section, we briefly review the method to extract multipole modes from a LWD system with an asymmetric source and four receiver arrays. The direct acoustic potential excited by an *asymmetric* source, as shown in Tang and Cheng (2004), is expressed as

$$\Phi^{\mathrm{i}}(r, r_0, z, z_0, k, \omega)$$
$$= \frac{1}{\pi} \sum_{n=0}^{\infty} \varepsilon_n \left\{ \begin{array}{ll} I_n(fr_0)K_n(fr), & r > r_0 \\ I_n(fr)K_n(fr_0), & r < r_0 \end{array} \right\}$$
$$\times cos(n(\theta - \theta_0))e^{ik(z-z_0)} \qquad (1)$$

by applying the Bessel addition theorem (Watson, 1944), where k is the axial wavenumber, ω is the angular frequency, r and r_0 are the receiver and source distance off the borehole center respectively, z and z_0 are the receiver and source position along z direction, θ_0 and θ are the azimuthal angles of the source and receiver. The radial wavenumber f is equal to $\sqrt{k^2 - (\omega/c_f)^2}$, where c_f is the fluid velocity. Similar to Φ^{i}, the scattered potential(Tang and Cheng, 2004) off the boundaries can be written as

$$\Phi^{\mathrm{sca}}(k, \omega) = \sum_{n=0}^{\infty} (D_n I_n(fr) + E_n K_n(fr)) cos(n(\theta - \theta_0))e^{ik(z-z_0)},$$

where D_n and E_n can be determined by matching the boundary conditions. The total potential $\Phi^{\mathrm{tot}}(k, \omega)$ in the borehole is the sum of the direct and the scattered potentials. We can calculate the dispersion curve (modal phase velocity versus frequencies) for the multipole modes, by searching the local maximum value of $\Phi^{\mathrm{tot}}(k, \omega)$ in the frequency-wavenumber domain.

When an asymmetric source is in the borehole, all modes are simultaneously excited, and receiver arrays over a range of azimuthal directions are required to resolve each individual mode. With four receivers distributed at 0°, 90°, 180° and 270° azimuthal angles, which is the case with our LWD tool (shown on Figure 1), we approximately resolve the monopole, dipole and quadrupole modes by neglect all higher order modes. The total potentials at these four receivers can be expressed as

$$\Phi_{\mathrm{r1}}^{\mathrm{tot}}(\theta = 0) = M + D + Q + \varepsilon;$$
$$\Phi_{\mathrm{r2}}^{\mathrm{tot}}(\theta = \pi/2) = M - Q + \varepsilon;$$
$$\Phi_{\mathrm{r3}}^{\mathrm{tot}}(\theta = \pi) = M - D + Q + \varepsilon;$$
$$\Phi_{\mathrm{r4}}^{\mathrm{tot}}(\theta = 3\pi/2) = M - Q + \varepsilon, \qquad (3)$$

where the source is put at 0° azimuthal angle without losing generality, M, D and Q are the total potential of monopole, dipole and quadrupole modes and ε is the sum of higher order potential. By adding and subtracting the potentials expressed in Eq. 3, the potentials of the monopole, dipole and quadrupole modes are

$$\Phi^{\mathrm{mono}} = \Phi_{\mathrm{r1}}^{\mathrm{tot}} + \Phi_{\mathrm{r2}}^{\mathrm{tot}} + \Phi_{\mathrm{r3}}^{\mathrm{tot}} + \Phi_{\mathrm{r4}}^{\mathrm{tot}},$$
$$\Phi^{\mathrm{di}} = \Phi_{\mathrm{r1}}^{\mathrm{tot}} - \Phi_{\mathrm{r3}}^{\mathrm{tot}},$$
$$\Phi^{\mathrm{quadru}} = \Phi_{\mathrm{r1}}^{\mathrm{tot}} - \Phi_{\mathrm{r2}}^{\mathrm{tot}} + \Phi_{\mathrm{r3}}^{\mathrm{tot}} - \Phi_{\mathrm{r4}}^{\mathrm{tot}}. \qquad (4)$$

We could also resolve hexapole, octupole and higher modes if given more receivers symmetrically distributed over the azimuthal direction.

NUMERICAL MODELING AND LABORATORY MEASUREMENTS

In this section, we investigate the acoustic field of the monopole, dipole and quadrupole modes excited by an asymmetric source in a borehole from numerical modelings and laboratory measurements. We perform a frequency-velocity dispersion analysis on synthetic and measured time traces for both slow and fast formation.
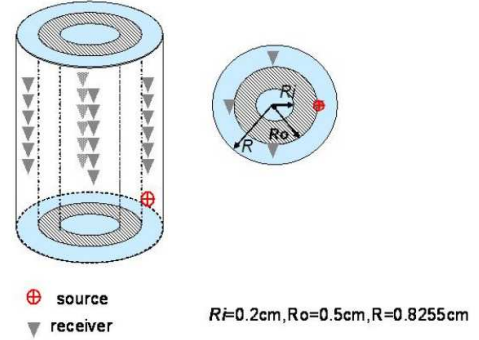

Figure 1: The geometry of borehole, positions of the source, receiver and LWD tool.

The geometry of the borehole, positions of the source, receivers and the scaled LWD tool used in this paper is shown in Figure 1. A detailed description of this acoustic tool can be found in Zhu *et al* (2008). The isotropic slow and fast formation surrounding the borehole is simulated by Lucite (Zhu *et al* 2008) and Berea Sandstone respectively. Other parameters including densities, shear and compressional velocities of the tool, fluid in the borehole, Lucite and Berea Sandstone are contained in Table. 1. A single-cycle sinusoidal source waveform centered at 50 kHz is used in all the laboratory measurements. Since the monopole mode can not be effectively excited by this source waveform, we will exclude the monopole mode and only use dipole and quadrupole modes in the following formation velocity inversion.

	Lucite	Berea Sandstone	Tool	Fluid
$V_p(m/s)$	2700	4660	4800	1480
$V_s(m/s)$	1290	2640	2400	0
$\rho(kg/m^3)$	1180	2200	4800	1000

Table 1: Parameters of fluid, formation and tool

Slow formation simulated by Lucite
We use a method developed by Rao and Toksoz (2005) to perform the dispersion analysis on dipole and quadrupole mode. This method includes the following steps:

(1) Fourier transform the received array time series into the frequency domain.
(2) For a given frequency ω_l, use a Gaussian window to weight the frequency spectrum over a given frequency interval centered at ω_l.
(3) Inverse Fourier transform the weighted spectrum to obtain "narrow-band" time series.
(4) Use the same non-dispersive time semblance analysis by Kimball (1986) on the new time series to obtain the phase velocity at frequency ω_l.

Figure. 2(a) shows the dispersion curves of the dipole mode calculated from synthetic and measured time traces, where the theoretical dispersion curve, represented by white circles, is calculated by searching for the local maximum values of $\Phi^{\text{tot}}(k,\omega)$. The estimated dispersion curve, as represented by black stars, is obtained through searching for the local maximum values of Fig. 2(a) for each frequency. Figure. 2(b) shows the estimated dispersion curve from the measured time traces. The energy and coherence of the tool mode is so strong that it totally masks the dipole mode at frequencies below 40kHz. This makes it is impossible to detect any dipole modes. For frequencies higher than 40kHz, the coherence of the dipole mode is still very weak compared to the tool mode although its amplitude is already larger. The amplitude of the tool mode is much larger than that of dipole mode at frequencies below 35kHz and vice-versa at frequencies higher than 40kHz, as shown in Figure. 2(c). In order to make use of the coherence and relatively large amplitude of the dipole mode simultaneously, we modify the non-dispersive time semblance analysis by Kimball (1986). Instead of calculating the coherence function defined in Eq. 3.8 of Tang and Cheng (2004)

$$\rho(s,T) = \frac{\int_T^{T+T_w} \left| \sum_{m=1}^N X_m(t+s(m-1)d) \right|^2 \mathrm{d}t}{N \sum_{m=1}^N \int_T^{T+T_w} |X_m(t+s(m-1)d)|^2 \mathrm{d}t} \quad (5)$$

where $X_m(t)$ is the acoustic time signal at the mth receiver in the array of N receivers, with a receiver spacing d, we use

$$\rho(s,T) = \int_T^{T+T_w} \left| \sum_{m=1}^N X_m(t+s(m-1)d) \right|^2 \mathrm{d}t \quad (6)$$

to take advantage of the relatively large amplitude of dipole mode at higher frequencies. As shown in Figure. 2(d), the dipole mode now can be identified separately from the tool mode and other background "noise" at frequency higher than 40kHz.

Figure. 3(a) shows the dispersion curve for the quadrupole mode including the leaky modes whose velocity are larger than the formation shear velocity. For the laboratory measurement, the energy in the leaky mode is so small that we can barely record any signals and the dispersion curve is "cut-off" at the formation shear velocity, as shown in Figure. 3(b). The estimated dispersion curve seems higher than the theoretical one for the laboratory measurements, as shown in Fig. 3(b). This difference leads to a higher estimated shear formation velocity.

Fast formalation simulated by Berea sandstone
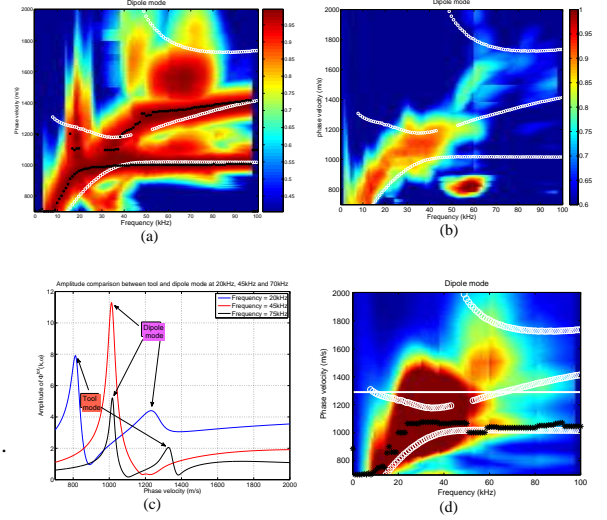We apply the same procedures described in Sec. to calculate

Figure 2: Dispersion curves of the (a) modeled and (b) measured dipole mode in the slow formation. (c) The amplitude of the total potential field at freqency 20 kHz, 45 kHz and 75 kHz. The dispersion curve shown on (d) is based on a weighted coherence function expressed in Eq. 6. White circles represent the theoretical calculations and black stars represent the local maximum values of the coherence functions.

the dispersion cuver for the dipole and quadrupole modes for a fast formation (Berea Sandstone). Figures. 4(a) and 4(b) shows the dispersion curves of the dipole mode from both synthetic and measured waveforms as well as the theoritical calculations. A very good match is found between the theoretical calculations (white circles) and both synthetic and laboratory measurements (black starts). The higher order dipole mode can also be seen clearly at 90 kHz to 100 kHz in the laboratory measurements, which could potentially be included in the dispersion curve fit for sheal estimation. Figures. 5(a) and 5(b) shows the dispersion curve of quadrupole mode. We find the dispersion curve from estimations of both synthetics and the measurments are slower than the theoretical calculation and the match is not as good as the dipole mode.
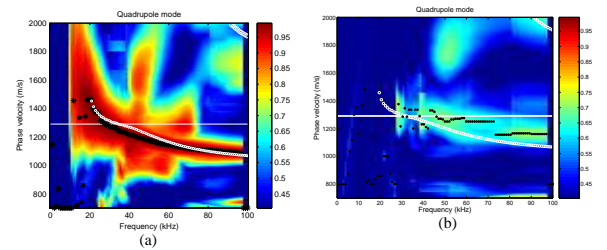

Figure 3: Dispersion curves of the quadrupole mode in the slow formation for (a) numerical modeling (b) laboratory measurements. White circles represent the theoretical calculations and black stars represent the local maximum values of the coherence functions.
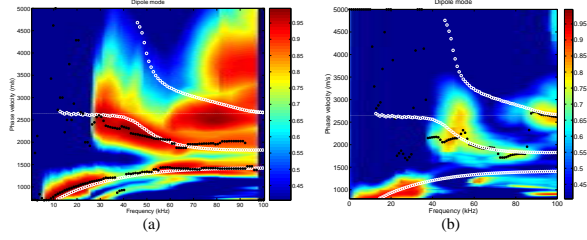
Figure 4: Dispersion curves of the dipole mode in the fast formation for (a) numerical modeling (b) laboratory measurements. White circles represent the theoretical calculations and black stars represent the local maximum values of the coherence functions.

RESULTS AND DISCUSSION

We apply the method of least square fitting to estimate the formation shear velocity from measured. For both dipole and quadrupole mode measurements, we first apply a band-pass filter to minimize the effects from tools mode. The best estimation of formation shear velocity is the one whose sum of squared velocity residuals over a desired frequency range has the least value, where the residual is defined as the phase velocity difference between the laboratory measurements and the theoretical calculations. We apply this least square fitting to both dipole and quadrupole mode measurements for the soft formation and only to dipole measurement for the hard formation. For quadrupole mode in the hard formation, we define the residual as the phase velocity difference between the laboratory measurements and the synthetics instead of the theoretical calculations. This is because the dispersion curve estimated from synthetic data can better capture the dispersion characteristics of quadrupole mode compared to the theoretical calculation, as shown in Fig. 5(c).

Slow formation
Figure. 6(a) shows the root of square velocity residuals as a function of the assumed formation shear velocity for the dipole and quadrupole mode. It is found that, the best estimates of the formation shear velocities are 1335 m/s (dipole), and 1360 m/s (quadrupole), respectively. Both of them are larger compared to the true formation velocity of 1290 m/s . When compared to the dipole measurements, the quadrupole measurements have larger residuals. We compute the best estimate for the shear velocity (1347.5 m/s) by averaging the values from dipole and quadrupole estimates. Using both dipole and quadrupole estimates simultaneously may sacrifice some accuracy under certain scenarios, ??? this case, where the dipole value is closer to the true velocity. However, it provides greater confidence and reduce the ambiguity in shear velocity estimation since it utilizes two independent measurements.

Fast formation
Figure. 6(b) shows the root of square velocity residuals for the dipole and quadrupole modes, but for the fast formation (Berea Sandstone), where the best estimates of the shear velocity is 2650 m/s (dipole) and 2500 m/s (quadrupole) respectively. The true velocity is 2640 m/s. The resolution of quadrupole resid-
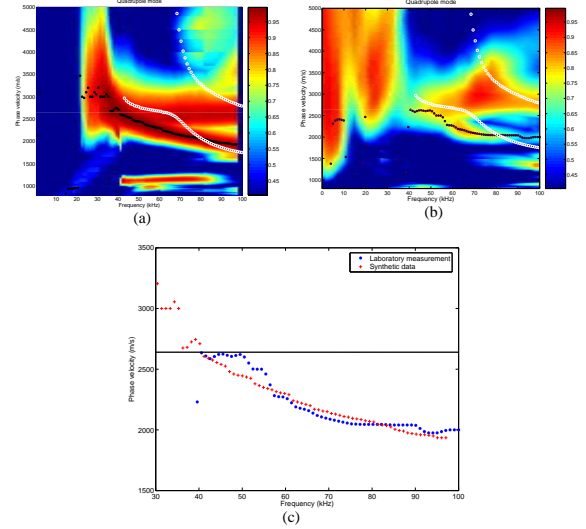

Figure 5: Dispersion curves of the quadrupole mode in the fast formation for (a) numerical modeling (b) laboratory measurements. (c) Dispersion curve estimated from laboratory measurements and synthetic data. White circles represent the theoretical calculations and black stars represent the local maximum values of the coherence functions in Figure (a) and (b).
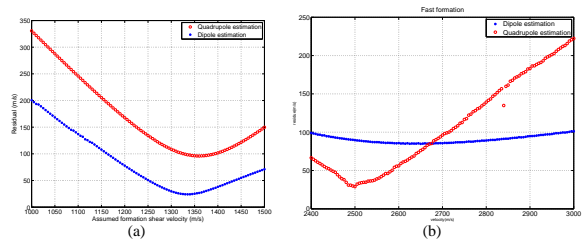

Figure 6: Squared velocity residual versus the assumed formation shear velocity for the dipole and quadrupole mode in the (a) slow formation, (b) fast formation

ual minumum is much better than the dipole although its estimation error, which is the difference between the estimated shear velocity and the ture value, is larger than the one from dipole. The velocity estimate by combining both dipole and quadropole is 2575 m/s.

CONCLUSION

In this paper, we show that the concept of asymmetric source logging could improve shear velocity estimates compared to traditional single mode methods. We demonstrate that, by adding and subtracting recorded signals from four-receiver arrays, we are able to extract and separate monopole, dipole and quadrupole modes simultaneously excited by an asymmetric source. When using both dipole and quadrupole modes, we effectively utilize two independence measurements to estimate the formation shear velocity, which could reduce ambiguity and improve the confidence of the estimation.

Reference

V. Briggs, R. Rao, S. Grandi, D. Burns, and S. Chi, 2004, A comparison of LWD and wireline dipole sonic data: Annual report of borehole acoustics and logging and reservoir delineation consortia, Massachusetts Institute of Technology.

J. Byun, M. N. Toksoz, and R. Rao, 2004, Effects of source mismatch on multipole logging: Annual report of borehole acoustics and logging and reservoir delineation consortia, Massachusetts Institute of Technology.

J. Byun and M. N. Toksoz, 2006, Effects of an off-centered tool on dipole and quadrupole logging: Geophysics, **71**, 91-99

C. V. Kimball and T. L. Marzetta, 1986, Semblance processing of borehole acoustic array data: Geophysics, **49**, 274-281

B. Nolte and X. J. Huang, 1997, Dispersion analysis of split flexural waves: Annual report of borehole acoustics and logging and reservoir delineation consortia, Massachusetts Institute of Technology.

R. Rao, D. R. Burns, and M. N. Toksoz, 1999, Models in LWD Applications: Annual report of borehole acoustics and logging and reservoir delineation consortia, Massachusetts Institute of Technology.

R. Rao. V. N. and M. N. Toksoz, 2005, Dispersive Wave Analysis - Method and Applications, Annual report of borehole acoustics and logging and reservoir delineation consortia, Massachusetts Institute of Technology.

X. M. Tang and A. Cheng, 2004, Quantitative borehole acoustic methods, Elsevier press.

G. A. Watson, 1944, A treatise on the theory of Bessel functions, Cambridge University press, second edition.

Z. Zhu, M. N. Toksoz, R. Rao and D. R. Burns, 2008, Experimental studies of monopole, dipole, and quadrupole acoustic logging while drilling (LWD) with scaled borehole models: Geophysics, **73**, 133-143